

## Accepted Manuscript

Discovery of NR2B-selective antagonists via scaffold hopping and pharmacokinetic profile optimization

Kosuke Anan, Moriyasu Masui, Aya Tazawa, Minoru Tomida, Yoshihiro Haga, Masaharu Kume, Shoichi Yamamoto, Shunji Shinohara, Hiroki Tsuji, Shinji Shimada, Shigenori Yagi, Nobuyoshi Hasebe, Hiroyuki Kai

PII: S0960-894X(19)30091-5  
DOI: <https://doi.org/10.1016/j.bmcl.2019.02.017>  
Reference: BMCL 26297

To appear in: *Bioorganic & Medicinal Chemistry Letters*

Received Date: 31 October 2018  
Revised Date: 25 January 2019  
Accepted Date: 14 February 2019

Please cite this article as: Anan, K., Masui, M., Tazawa, A., Tomida, M., Haga, Y., Kume, M., Yamamoto, S., Shinohara, S., Tsuji, H., Shimada, S., Yagi, S., Hasebe, N., Kai, H., Discovery of NR2B-selective antagonists via scaffold hopping and pharmacokinetic profile optimization, *Bioorganic & Medicinal Chemistry Letters* (2019), doi: <https://doi.org/10.1016/j.bmcl.2019.02.017>

This is a PDF file of an unedited manuscript that has been accepted for publication. As a service to our customers we are providing this early version of the manuscript. The manuscript will undergo copyediting, typesetting, and review of the resulting proof before it is published in its final form. Please note that during the production process errors may be discovered which could affect the content, and all legal disclaimers that apply to the journal pertain.



## Discovery of NR2B-selective antagonists via scaffold hopping and pharmacokinetic profile optimization

Kosuke Anan,<sup>a\*</sup> Moriyasu Masui,<sup>a</sup> Aya Tazawa,<sup>a</sup> Minoru Tomida,<sup>a</sup> Yoshihiro Haga,<sup>a</sup> Masaharu Kume,<sup>a</sup> Shoichi Yamamoto,<sup>b</sup> Shunji Shinohara,<sup>d</sup> Hiroki Tsuji,<sup>d</sup> Shinji Shimada,<sup>d</sup> Shigenori Yagi,<sup>c</sup> Nobuyoshi Hasebe,<sup>c</sup> and Hiroyuki Kai<sup>a</sup>

<sup>a</sup> Medicinal Chemistry Research Laboratory, Shionogi & Co., Ltd, 1-1 Futabacho, 3-chome, Toyonaka 561-0825, Japan

<sup>b</sup> Drug Discovery & Disease Research Laboratory, Shionogi & Co., Ltd, 1-1 Futabacho, 3-chome, Toyonaka 561-0825, Japan

<sup>c</sup> Research Laboratory for Development, Shionogi & Co., Ltd, 1-1 Futabacho, 3-chome, Toyonaka 561-0825, Japan

<sup>d</sup> Shionogi Techno Advance Research Co., Ltd., 1-1 Futabacho, 3-chome, Toyonaka 561-0825, Japan

\*Corresponding author. Tel.: +81 (6) 6331 5833; fax: +81 (6) 6332 6385. E-mail address: kousuke.anan@shionogi.co.jp (K. Anan)

**Keywords:** NMDA receptor antagonist; scaffold hopping; analgesic activity

### Abstract

Selective *N*-methyl-D-aspartate receptor subunit 2B (NR2B) antagonists show potential as analgesic drugs, and do not cause side effects associated with non-selective *N*-methyl-D-aspartate (NMDA) antagonists. Using a scaffold-hopping approach, we previously identified isoxazole derivative **4** as a potent selective NR2B antagonist. In this study, further scaffold hopping of isoxazole derivative **4** and optimization of its pharmacokinetic profile led to the discovery of the orally bioavailable compound **6v**. In a rat study of analgesia, **6v** demonstrated analgesic effects against neuropathic pain.

### Text body

The *N*-methyl-D-aspartate (NMDA) receptor (NR), a glutamic acid receptor, is highly expressed throughout the central nervous system.<sup>1</sup> The NR is a heterotetrameric complex composed of the three subunits NR1 (a-h), NR2 (A-D), and NR3 (A-B), and is activated by the amino acids glutamate and glycine.<sup>2,3</sup> The NMDA receptor subunit 2A (NR2A) is involved in memory formation and learning acquisition, whereas excessive activation of the NMDA receptor subunit 2B (NR2B) results in neurodegenerative cell death and transmission of pain related to brain ischemia.<sup>4</sup> Studies investigating mice overexpressing NR2B have revealed its important role in pain.<sup>5</sup> Because of the restricted distribution of NR2B to the forebrain and spinal cord dorsal horn, NR2B-selective antagonists may reduce side effects associated with the use of non-selective antagonists.<sup>6</sup> This evidence points to the use of selective NR2B antagonists as a promising strategy in the development

of novel analgesics.

In a previous report, we introduced the use of a scaffold-hopping approach to develop a new selective NR2B antagonist, by utilizing the structure of a known compound.<sup>7</sup> Considering the improved inhibitory activity against human ether-à-go-go-related gene (hERG) channels conferred by the structure of the selective NR2B antagonist radiprodil (**1**)<sup>8</sup> and compound **2** (Pfizer),<sup>9,10</sup> we designed the acetamide derivative **3** by hybridizing the side-chain in compound **1** and the cyclohexanol ring in compound **2**. Compound **3** showed high *in vitro* potency, but unfortunately displayed low brain penetration. To improve brain penetration, this series was further optimized via replacement of the amide in compound **3** with an isoxazole, and efforts to optimize the pharmacokinetic profiles led to the discovery of the orally available brain penetrant compound **4**, which displayed analgesic activity in mice.

In this study, we designed the novel isoxazole derivative **5**, in which the cyclohexanol ring in compound **4** was converted via scaffold hopping to create a chemotype with improved pharmacokinetics. Although isoxazole derivative **5** showed potent activity as expected, its pharmacokinetic profile was unsatisfactory. Next, we developed the novel oxamide derivative **6**, in which the isoxazole ring was converted to an amide. Certain derivative compounds maintained high activity, showed improved pharmacokinetic profiles, and exerted strong analgesic effects in a rat model of neuropathic pain. Here, we describe our efforts to identify the novel isoxazole derivative **5** and oxamide derivative **6**.

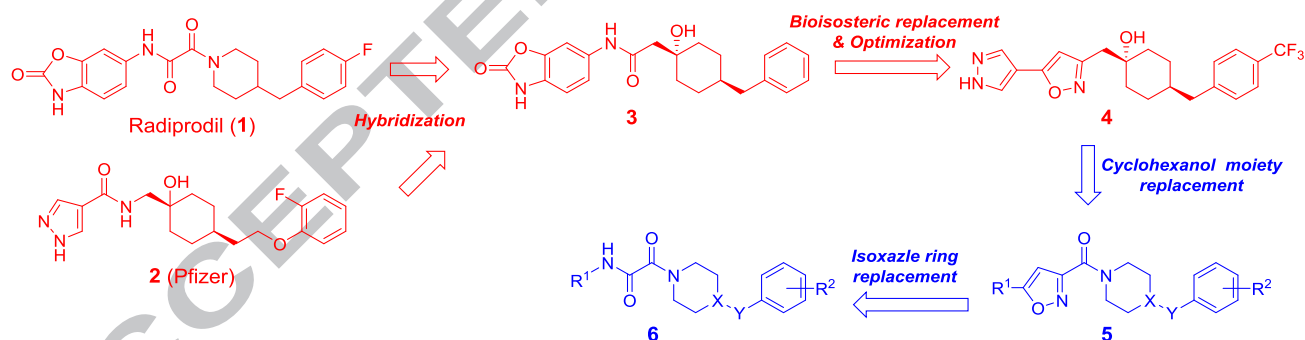
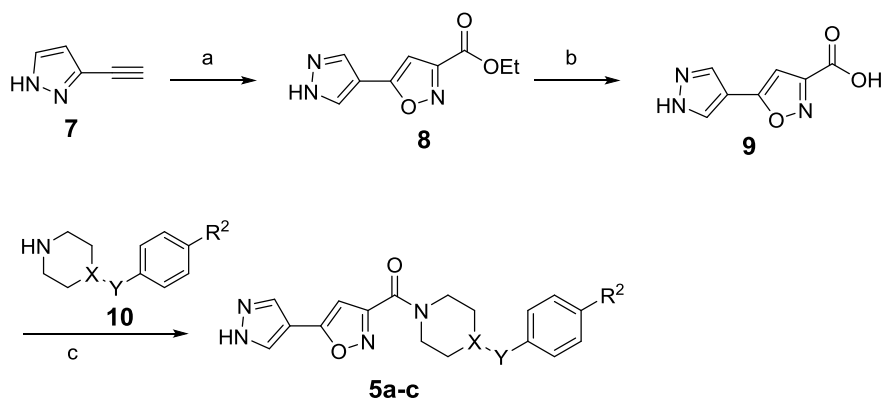


**Figure 1.** Summary of compounds described in previous reports (red) and in this report (blue)

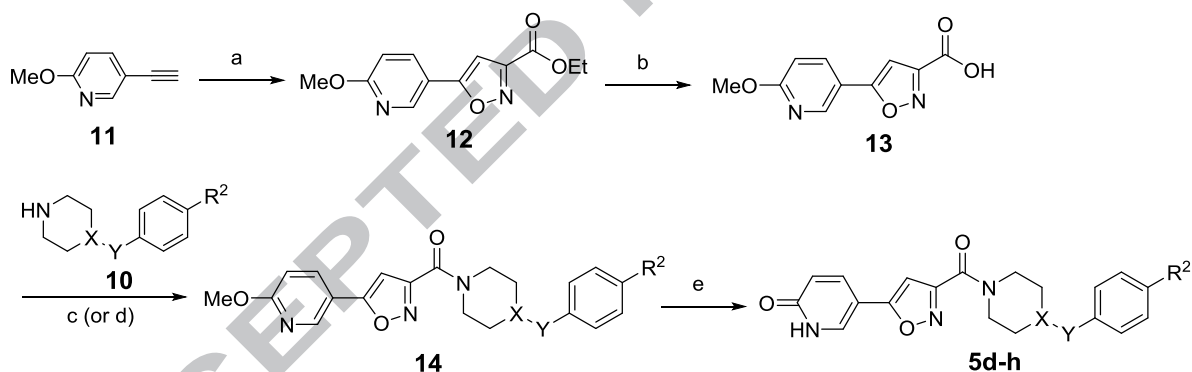
The syntheses of pyrazoles **5a-c** (Scheme 1) started with 3-ethynyl-1*H*-pyrazole (**7**), which was treated with ethyl 2-chloro-2-hydroxyiminoacetate to produce ester **8**. Hydrolysis of ester **8** following amide coupling with corresponding amines **10** yielded pyrazoles **5a-c**. Amine **10** was commercially available or prepared from commercially available starting materials following standard procedures.<sup>11</sup>



### Scheme 1. Synthesis of pyrazoles **5a-c**

Reagents and conditions: (a) Ethyl 2-chloro-2-hydroxyiminoacetate,  $\text{NaHCO}_3$ , *i*-PrOH, room temperature (rt) 3 days, yield: 76%; (b) 2M-NaOH *aq.*, MeOH, rt 2 h, 75%; (c) **10**·HCl, HOBT, DMAP, WSCD·HCl,  $\text{Et}_3\text{N}$ , DMF, rt 2 h, 69-90%.

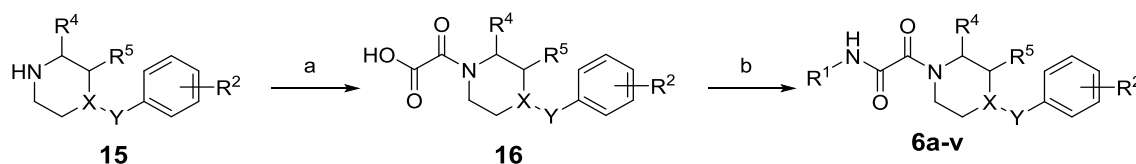
The pyridones **5d-h** (Scheme 2) were prepared from 5-ethynyl-2-methoxypyridine (**11**) via synthetic methods similar to those depicted in Scheme 1. Removal of a methyl group from **14** yielded the pyridones **5d-h**.



### Scheme 2. Synthesis of pyridones **5d-h**

Reagents and conditions: (a) Ethyl 2-chloro-2-hydroxyiminoacetate,  $\text{NaHCO}_3$ , *i*-PrOH, 40 °C 24 h, 80%; (b) 2M-NaOH *aq.*, MeOH, rt 2 h, quant.; (c) **10**·HCl, HOBT, DMAP, WSCD·HCl,  $\text{Et}_3\text{N}$ , DMF, rt 2 h, 91-97%; (d)  $(\text{COCl})_2$ , dimethylformamide (DMF, *cat.*), tetrahydrofuran (THF), reflux 2 h, then **10**·HCl, pyridine, THF, rt 3 h, 69-94%; (e) Trimethylsilyl chloride (TMSCl), NaI, MeCN, reflux 2 h, 20-91%.

The oxamide derivatives **6a-v** were prepared according to the method depicted in Scheme 3. Amide coupling of amine **15** with ethyl 2-chloro-2-oxoacetate followed by hydrolysis yielded the carboxylic acid **16**. Amine **15** was commercially available or synthesized according to reported procedures.<sup>12</sup> Finally, amide coupling of **21** with anilines produced oxoamide derivatives **6a-v**.



**Scheme 3.** Synthesis of oxamide **6a-v**

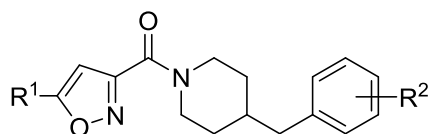
Reagents and conditions: (a) ClCOCO<sub>2</sub>Et, Et<sub>3</sub>N, CH<sub>2</sub>Cl<sub>2</sub>, 0 °C 0.5-1 h, 80-99%; then 2M-NaOH aq., EtOH, rt 1.5 h, 77-99%; (c) R<sup>1</sup>-NH<sub>2</sub>, HOBt, DMAP, WSCD·HCl, Et<sub>3</sub>N, DMF, rt overnight, 46-91%.

Compounds were assessed via an NR2B-selective binding assay<sup>13</sup> using the radiolabeled ligand [<sup>3</sup>H]-ifenprodil, an NR1/NR2B-specific antagonist. Compounds active in this test were then evaluated in a functional assay<sup>14</sup> to assess the level of inhibition of Ca ion influx in NR-overexpressing human embryonic kidney (HEK) 293 cells. A positive correlation between binding and functional inhibitory potency was observed. Compounds **5a-f**, in which the cyclohexanol ring in compound **4** was substituted with a piperidine ring, were investigated (Table 1). All compounds displayed potent binding and antagonistic activities, especially compound **5f**, which was more potent than compound **4** and radiprodil (**1**). Conversion of the cyclohexanol ring in compound **4** to a piperidine ring had no significant influence on the activity of the compounds. The amide moiety present in radiprodil (**1**) is converted to an isoxazole ring in compounds **5a-f**, and considering both the present results and those of previous reports,<sup>7,15,16</sup> both the amide moiety and isoxazole ring are assumed to be bioisosteres.

The rat pharmacokinetic studies of the compounds described in Table 1 (with the exception of **5b**) were conducted in male Sprague-Dawley (SD) rats with intravenous (iv) and oral administration of 0.5 and 1 mg/kg doses, respectively. Although the pyrazole-type compounds **5a** and **5c** showed high brain partition coefficients (*K<sub>p</sub>*), their total clearance and bioavailability were low. In contrast, although the pyridine-type compounds **5d-f** showed lower brain *K<sub>p</sub>* than the pyrazoles, their total clearance and bioavailability were acceptable. However, none of the compounds (**5a** and **5c-f**) showed comparable pharmacokinetic profiles to that of compound **4**. Because radiprodil (**1**) also displayed a high total clearance, these results suggest that the piperidine ring may be responsible for the poor pharmacokinetic profiles displayed by the compound series **5**.

**Table 1.** Structure-activity derivatives **5a-f**

relationships (SARs) of isoxazole



Compound No	R <sup>1</sup>	R <sup>2</sup>	NR2B (bind) <sup>a</sup> pIC <sub>50</sub>	NR2B(Ca <sup>2+</sup> ) <sup>b</sup> pIC <sub>50</sub>	CLt <sup>c</sup> (mL/min/kg)	F <sup>c</sup> (%)	Brain <i>K<sub>p</sub></i> <sup>d</sup>
<b>5a</b>		H	7.1	7.3	71.6	0.2	3.89
<b>5b</b>		4-F	7.1	7.2	NT	NT	NT
<b>5c</b>		4-Cl	7.2	7.4	29.2	0.6	3.27
<b>5d</b>		H	7.2	7.2	19.3	18.4	0.37
<b>5e</b>		4-F	7.3	7.4	19.7	18.4	0.50
<b>5f</b>		4-Cl	7.6	8.0	5.4	9.3	0.38
<b>radiprodil (1)</b>			7.5	8.5	37.1	30.0	1.00
<b>4</b>			7.0	7.9	4.0	67.5	2.66

<sup>a</sup> Inhibition of binding of [<sup>3</sup>H]-ifenprodil to rat brain membranes

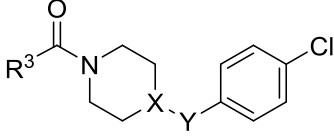
<sup>b</sup> Inhibition of Ca ion influx in mouse *N*-methyl-D-aspartate (NMDA) receptor-overexpressing HEK293 cells

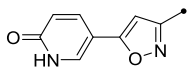
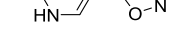
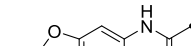
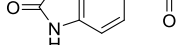
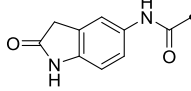
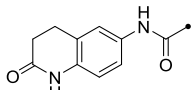
<sup>c</sup> CLt = total clearance; *F* = bioavailability. Compounds were administered at doses of 0.5 mg/kg (intravenous injection, iv) and 1.0 mg/kg (oral) using a cassette dosing method.

<sup>d</sup> Brain *K<sub>p</sub>* = total brain-to-plasma ratio. Plasma and brain samples were collected 0.5 h after iv administration of a 0.5-mg/kg dose using a cassette dosing method.

NR2B, *N*-methyl-D-aspartate receptor subunit 2B; pIC<sub>50</sub>, negative log of the 50% inhibitory concentration, -log(IC<sub>50</sub>); NT = not tested

To improve the pharmacokinetic profiles of compounds **5**, the piperidine ring in compound **5f** was converted, resulting in compounds **5g** and **5h** (Table 2). Unfortunately, piperazine derivatives **5g** and **5h** showed reduced binding activity. However, a similar conversion was conducted on radiprodil (**1**), yielding the benzyl piperazine **6a** which showed reduced activity, and the phenylpiperazine **6b** which showed increased activity. In rat pharmacokinetic studies, **6a** and **6b** showed lower total clearance than radiprodil (**1**). Furthermore, the benzoxazolone ring in **6b** was converted to an indolone ring or a dihydroquinolone ring, which showed high activity in our previous study.<sup>7</sup> Compounds **6c** and **6d** showed greatly decreased binding activity. From the piperazine derivatives described above, only **6b** showed high activity.

**Table 2.** SARs of piperidine linker moieties **5f-h** and **6a-d**


Compound No	R <sup>3</sup>	X	Y	NR2B (bind) <sup>a</sup> pIC <sub>50</sub>	NR2B(Ca <sup>2+</sup> ) <sup>b</sup> pIC <sub>50</sub>	CLt <sup>c</sup> (mL/min/kg)	F <sup>c</sup> (%)	Brain <i>K<sub>p</sub></i> <sup>d</sup>
<b>5f</b>		CH <sub>2</sub>	CH <sub>2</sub>	7.6	8.0	5.4	9.3	0.38
<b>5g</b>		N	CH <sub>2</sub>	< 6.0	NT	NT	NT	NT
<b>5h</b>		N	None	< 6.0	NT	NT	NT	NT
<b>1</b>		CH <sub>2</sub>	CH <sub>2</sub>	7.5	8.5	37.1	30.0	1.00
<b>6a</b>		N	CH <sub>2</sub>	6.3	7.2	6.8	7.4	0.41
<b>6b</b>		N	None	7.8	8.1	7.2	17.8	0.53
<b>6c</b>		N	None	< 6.0	NT	NT	NT	NT
<b>6d</b>		N	None	< 6.0	NT	NT	NT	NT

<sup>a</sup> Inhibition of binding of [<sup>3</sup>H]-ifenprodil to rat brain membranes

<sup>b</sup> Inhibition of Ca<sup>2+</sup> ion influx in mouse *N*-methyl-D-aspartate (NMDA) receptor-overexpressing HEK293 cells

<sup>c</sup> CLt = total clearance; *F* = bioavailability. Compounds were administered at doses of 0.5 mg/kg (intravenous injection, iv) and 1.0 mg/kg (oral) using a cassette dosing method.

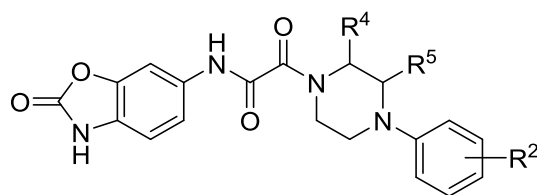
<sup>d</sup> Brain *K<sub>p</sub>* = total brain-to-plasma ratio. Plasma and brain samples were collected 0.5 h after iv administration of a 0.5-mg/kg dose using a cassette dosing method.

NR2B, *N*-methyl-D-aspartate receptor subunit 2B; pIC<sub>50</sub>, negative log of the 50% inhibitory concentration, -log(IC<sub>50</sub>); NT = not tested

Phenyl piperazine **6b**, which showed potent binding activity and an adequate pharmacokinetic profile, was identified as the lead compound via a scaffold-hopping approach. We next investigated R<sup>2</sup> substituents in **6b** (Table 3). Binding activity comparable to that of **6b** was observed in the compound with 4-CF<sub>3</sub> (**6g**), whereas reduced binding activity was observed with 4-F (**6f**) and 4-MeO

(6h). Removal of the R<sup>2</sup> substituent (6e) caused diminished binding activity. In addition, the activities of 3,4-disubstituted compounds (6i, 6k-n) were comparable to those of 4-substituted compounds, whereas the activity of the 3,5-disubstituted compound (6j) was reduced. Among 3,4-disubstituted compounds, those with 3-F-4-Cl (6l) and 3-F-4-CF<sub>3</sub> (6m) displayed the most potent antagonistic activities. In rat pharmacokinetic studies of these compounds, 6l displayed a suitable pharmacokinetic profile. Total clearance of the compound with 3-F-4-MeO (6n) was extremely high, and we therefore assume that the MeO group in 6n was the main metabolic point.

To improve pharmacokinetics profiles, the introduction of a methyl group into the piperazine ring was investigated.<sup>17</sup> Introduction of a methyl group with *R* configuration into the substituent R<sup>4</sup> (6o) resulted in binding activity comparable to that of 6b. Introduction of a methyl group with *S* configuration into the substituent R<sup>4</sup> (6p) caused diminished binding activity. Furthermore, when a methyl group was introduced into the substituent R<sup>5</sup>, 6q (*R* configuration) showed high activity whereas 6r (*S* configuration) displayed low binding activity. Compound 6o showed improved oral bioavailability compared to 6b, and 6q showed slightly higher total clearance than 6b, and much improved oral bioavailability and brain penetration. Therefore, a methyl group was introduced into the piperazine ring with R<sup>2</sup> (3,4-F<sub>2</sub> and 3-F-4-Cl). As a result, compounds 6s-v displayed improved pharmacokinetic profiles while maintaining high binding activity.

**Table 3.** SARs of phenylpiperazine derivatives **6b**, **e-v**

Comp ound No	R <sup>2</sup>	R <sup>4</sup>	R <sup>5</sup>	NR2B (bind) <sup>a</sup> pIC <sub>50</sub>	NR2B(Ca <sup>2+</sup> ) <sup>b</sup> pIC <sub>50</sub>	CLt <sup>c</sup> (mL/min/kg)	F <sup>c</sup> (%)	Brain <i>K<sub>p</sub></i> <sup>d</sup>
<b>6b</b>	4-Cl	H	H	7.8	8.1	7.2	17.8	0.53
<b>6e</b>	H	H	H	< 6.0	NT	NT	NT	NT
<b>6f</b>	4-F	H	H	6.9	6.9	11.1	39.3	NT
<b>6g</b>	4-CF <sub>3</sub>	H	H	7.6	8.2	15.1	24.8	2.99
<b>6h</b>	4-MeO	H	H	6.6	6.7	NT	NT	NT
<b>6i</b>	3,4-F <sub>2</sub>	H	H	7.7	8.0	4.0	13.0	0.82
<b>6j</b>	3,5-F <sub>2</sub>	H	H	6.8	7.0	NT	NT	NT
<b>6k</b>	3-Cl-4-F	H	H	7.5	8.0	18.3	24.6	1.24
<b>6l</b>	3-F-4-Cl	H	H	7.9	9.0	5.6	28.2	0.79
<b>6m</b>	3-F-4-CF <sub>3</sub>	H	H	7.8	9.0	5.6	8.7	0.65
<b>6n</b>	3-F-4-MeO	H	H	7.8	7.8	100.8	0.6	3.17
<b>6o</b>	4-Cl	( <i>R</i> )-Me	H	7.5	8.2	5.4	129.5	0.95
<b>6p</b>	4-Cl	( <i>S</i> )-Me	H	< 6.0	NT	NT	NT	NT
<b>6q</b>	4-Cl	H	( <i>R</i> )-Me	7.2	8.2	15.6	52.6	1.85
<b>6r</b>	4-Cl	H	( <i>S</i> )-Me	6.2	7.0	NT	NT	NT
<b>6s</b>	3,4-F <sub>2</sub>	( <i>R</i> )-Me	H	7.3	8.2	5.6	117.9	0.67
<b>6t</b>	3,4-F <sub>2</sub>	H	( <i>R</i> )-Me	7.2	8.0	15.9	25.3	1.89
<b>6u</b>	3-F-4-Cl	( <i>R</i> )-Me	H	7.9	8.7	1.37	30.4	0.99
<b>6v</b>	3-F-4-Cl	H	( <i>R</i> )-Me	7.3	8.5	6.0	32.0	1.19

<sup>a</sup> Inhibition of binding of [<sup>3</sup>H]-ifenprodil to rat brain membranes

<sup>b</sup> Inhibition of Ca ion influx in mouse *N*-methyl-D-aspartate (NMDA) receptor-overexpressing HEK293 cells

<sup>c</sup> CLt = total clearance; *F* = bioavailability. Compounds were administered at doses of 0.5 mg/kg (intravenous injection, iv) and 1.0 mg/kg (oral) using a cassette dosing method.

<sup>d</sup> Brain *K<sub>p</sub>* = total brain-to-plasma ratio. Plasma and brain samples were collected 0.5 h after iv administration of a 0.5-mg/kg dose using a cassette dosing method.

NR2B, *N*-methyl-D-aspartate receptor subunit 2B; pIC<sub>50</sub>, negative log of the 50% inhibitory concentration, -log(IC<sub>50</sub>); NT = not tested

Based on their favorable pharmacokinetic profiles, **6o**, **6u**, **6q**, and **6v** were subjected to an *in vivo* analgesic study. Their analgesic effects were evaluated after oral administration based on the change in pain threshold relative to allodynia (von Frey test) in a rat partial sciatic nerve ligation model.<sup>18</sup> Mechanical allodynia was quantified by measuring the hind paw withdrawal response to von Frey hair stimulation. The response before drug administration was measured (vehicle), and the evaluation was carried out 3 h after oral administration of each compound (2.5, 5, 10, and 20 mg/kg). The dose associated with an effect significantly different to that of the vehicle was considered the minimum effective dose (MED). As shown in Table 4, all compounds showed a significant increase in pain threshold at doses below 10 mg/kg. Among these compounds, **6v** demonstrated a significant analgesic effect at 2.5 mg/kg. Fortunately, the hERG inhibitory activity<sup>19</sup> of **6v** was lower than that of the other compounds (**6o**, **6u**, and **6q**).

**Table 4.** Biological activity and human ether-à-go-go-related gene (hERG) inhibitory activity of selected compounds

Compound	Analgesic effects <sup>a</sup>	hERG <sup>b</sup>	
	No	MED (mg/kg)	Inhibition at 1 $\mu$ M (%)
<b>6o</b>		10.0	36
<b>6q</b>		10.0	25
<b>6u</b>		5.0	29
<b>6v</b>		2.5	10

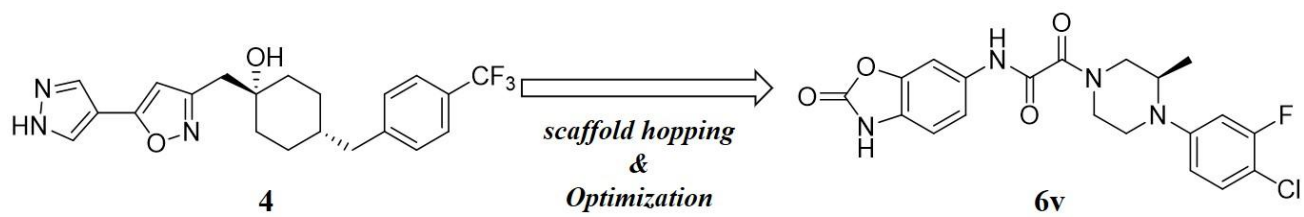
<sup>a</sup> Data were obtained from 10 rats per group and expressed as the minimum effective dose (MED) with antiallodynic effect;  $p < 0.01$  vs the vehicle.

<sup>b</sup> % inhibition at 1  $\mu$ M in human ether-à-go-go-related gene (hERG)-expressing HEK293 cells

In summary, the novel isoxazole derivative **5** was designed via a scaffold-hopping approach, starting with the previously identified NR2B-selective antagonist **4**. Although the compound series **5** exhibited high binding activity, pharmacokinetic profiles required improvement. Further optimization of **5** through bioisosteric replacement and efforts to optimize the pharmacokinetic profiles led to the discovery of **6v**, which demonstrated analgesic effects in the neuropathic pain model.

## References and notes

1. Banke, T. G., and Traynelis, S. F. *Nat. Neurosci.* 2003, 6, 144–152.
2. McBain, C. J., and Mayer, M. L. *Physiol. Rev.* 1994, 74, 723–760.
3. Bendel, O., Meijer, B., Hurd, Y., and Von Euler, G. *Neurosci. Lett.* 2005, 377, 31–36.
4. Parsons, C. G., Danysz, W., Quack, G. *Drug News Perspect.* 1998, 11, 523-69.
5. Wei, F., Wang, G.-D., Kerchner, G. A., Kim, S. J., Xu, H.-M., Chen, Z.-F., Zhuo, M. *Nat. Neurosci.* 2001, 4, 164-9.
6. Gogas, K. R. *Curr. Opin. Pharmacol.* 2006, 6, 68–74.
7. Anan, K., Masui, M., Hara, S., Ohara, M., Kume, M., Yamamoto, S., Shinohara., Tsuji, H., Shimada, S., Yagi, S., Hasebe, N., Kai, H. *Bio. Med. Chem. Lett.* 2017, 27, 4194-4198.
8. Mony, L., Kew, J. N., Gunthorpe, M. J., Paoletti, P. Br. *J. Pharmacol.* 2009, 157, 1301-1317.
9. McCauley, J. *Expert Opin. Ther. Patents.* 2006, 16, 863-870.
10. Kawai, M., Kawamura, M., Sakurada, I., Morita, A., (Pfizer, Inc.), WO2005080317.
11. Zhou, Z-L, and Keana, J. F. W, *J. Org. Chem.* 1999, 64, 3763-3766.
12. Smith, B., Tsai, J., Chen, R., (Arena Pharmaceuticals, Inc.), WO2005016902.
13. Masui, M., Adachi, M., Mikamiyama, H., Matsumura, A., Tsuno, N., (Shionogi & CO., LTD.), EP1988077A1, p 119.
14. Masui, M., Adachi, M., Mikamiyama, H., Matsumura, A., Tsuno, N., (Shionogi & CO., LTD.), EP1988077A1, p 121.
15. (a) Kai, H., Nakayama, K., Tsuji, H., Masuko, M., Takase, A. *J. Pesticide Sci.* 1998, 23, 44-48.  
(b) Kai, H., Ichiba, T., Miki, M., Takase, A., Masuko, M. *J. Pesticide Sci.* 1999, 24, 130-137.  
(c) Kai, H., Ichiba, T., Tomida, M., Masuko, M. *J. Pesticide Sci.* 1999, 24, 149-155.
16. (a) Meanwell, N. A. *J. Med. Chem.* 2011, 54, 2529-2591.  
(b) Zhiqing, L., Pingyuan, W., Haiying, C., Eric, A. W., Bing, T., Allan, R. B., Jia, Z. *J. Med. Chem.* 2017, 60, 4533-4558.
17. Eliezer, J. B., Arthur, E. K., Carlos, A. M. F. *Chem. Rev.* 2011, 111, 5215–5246.
18. Seltzer, Z., Dubner, R., Shir, Y. *Pain.* 1990, 43, 205–218.
19. Kai, H., Kameyama, T., Hasegawa, T., Oohara, M., Endoh, T., (Shionogi & CO., LTD.), EP2399910A1, p 219.



ACCEPTED MANUSCRIPT